Quenching of the Efficiency Droop in Cubic Phase InGaAlN Light-Emitting Diodes

Yi-Chia Tsai, Jean-Pierre Leburton, *Life Fellow, IEEE*, and Can Bayram, *Senior Member, IEEE*

***Abstract*— We show that the coexistence of strong internal polarization and large carrier (i.e., electron and hole) effective mass accounts for ∼51% of the efficiency droop under high current densities in traditional (hexagonal-phase) indium–gallium–aluminum–nitride (InGaAlN) light-emitting diodes (h-LEDs) compared to cubic-phase InGaAlN LEDs (c-LEDs). Our analysis based on variational technique on c-LEDs predicts an enhancement of the current density at the onset of the droop, inherently present in green c-LEDs. These effects are a consequence of the polarization-free nature and small carrier effective mass of c-LEDs. Our analysis indicates that, by overlooking the electron–hole wave function overlap, the well-known ABC model is suspected to overestimate the Auger coefficient, leading to questionable conclusions on the efficiency droop. In turn, it shows that the c-LED efficiency droop is much immune to the Auger electron–hole asymmetry, the increase in the Auger coefficient, and, thus, efficiency degradation mechanisms.**

***Index Terms*— Cubic phase, efficiency droop, InGaAlN, internal polarization, light-emitting diode (LED).**

I. Introduction

NOWADAYS, white light-emitting diodes (LEDs) can reach ∼200 lm/W while still generating more heat than light. According to the traditional solid-state lighting (SSL) roadmap, these phosphor-converted LEDs have a theoretical luminous efficacy limit of 255 lm/W [1]. However, in these white LEDs, phosphors and secondary lenses degrade significantly their source efficiency, optical delivery efficiency, and spectral efficacy [1], [2]. A new and accelerated SSL roadmap to achieve an ultimate luminous efficacy of 414 lm/W can only succeed via color-mixing phosphor-free direct-emitting LEDs [1]. Among the visible LEDs, green LEDs are four times less efficient than their blue counterparts and suffer the most from an efficiency droop (i.e., an efficiency rollover as the current density increases once the maximum internal quantum efficiency (IQE) has been reached). Auger recombination, electron leakage, and internal polarization are among the mechanisms proposed to explain this efficiency degradation. Recent experiments on traditional (hexagonal-phase) indium–gallium–aluminum–nitride (InGaAlN) LEDs (h-LEDs) reported hot-carrier emission from the InGaN quantum wells (QWs), implying strong Auger recombination, even under a low current density of ∼1.6 A/cm^2 [3]. The strong Auger recombination is typically attributed to a large Auger coefficient of 10^{-30} cm$^6 \cdot$s^{-1}, enhanced by phonon scattering [4], alloy scattering [4], and interface roughness scattering [5]. However, this explanation is inconsistent with the low-efficiency droop in gallium–arsenide (GaAs)- and gallium–phosphide (GaP)-based LEDs, which have similar Auger coefficients [6]–[8]. Moreover, in h-LEDs, the efficiency droop increases as the emission wavelength (and the indium mole fraction) increases from blue to green, which cannot be explained by the large Auger coefficient value alone.

In this article, the inherent causes of the efficiency droop and low current density at the onset of the efficiency droop in green h-LEDs and cubic-phase (instead of traditional, hexagonal-phase) InGaAlN LEDs (c-LEDs) are investigated by computational modeling. We find that the coexistence of strong internal polarization and large carrier (i.e., electron and hole) effective mass induces strong Auger recombination that causes the large performance rollover in h-LEDs. On the opposite, in c-LEDs, the absence of internal polarization together with smaller carrier effective mass weakens Auger recombination, which quenches the droop by ∼51%. These findings point at new ways to improve the performance of green LEDs.

II. Computational Details

For the sake of performance comparison, an h-LED and a c-LED are simulated with the following structure configuration: 120-nm-thick n-type GaN:Si [Si concentration of 10^{18} cm^{-3}]/10-nm-thick i-GaN barrier/3-nm i-$In_{0.30}Ga_{0.70}N$ single QW/10-nm-thick i-GaN

Manuscript received March 9, 2022; revised April 6, 2022; accepted April 12, 2022. This work was supported in part by the National Science Foundation Faculty Early Career Development Program (CAREER) under Award NSF-ECCS-16–52871 and in part by the Extreme Science and Engineering Discovery Environment (XSEDE, computational resources allocated) under Grant TG-DMR180075. The review of this article was arranged by Editor G. Ghione. *(Corresponding author: Can Bayram.)*

Yi-Chia Tsai and Can Bayram are with the Department of Electrical and Computer Engineering, University of Illinois at Urbana–Champaign, Urbana, IL 61801 USA, and also with the Holonyak Micro and Nanotechnology Laboratory, University of Illinois at Urbana–Champaign, Urbana, IL 61801 USA (e-mail: yichiat2@illinois.edu; cbayram@illinois.edu).

Jean-Pierre Leburton is with the Department of Electrical and Computer Engineering, University of Illinois at Urbana–Champaign, Urbana, IL 61801 USA, also with the Holonyak Micro and Nanotechnology Laboratory, University of Illinois at Urbana–Champaign, Urbana, IL 61801 USA, and also with the Department of Physics, University of Illinois at Urbana–Champaign, Urbana, IL 61801 USA (e-mail: jleburto@illinois.edu).

Color versions of one or more figures in this article are available at https://doi.org/10.1109/TED.2022.3167645.

Digital Object Identifier 10.1109/TED.2022.3167645

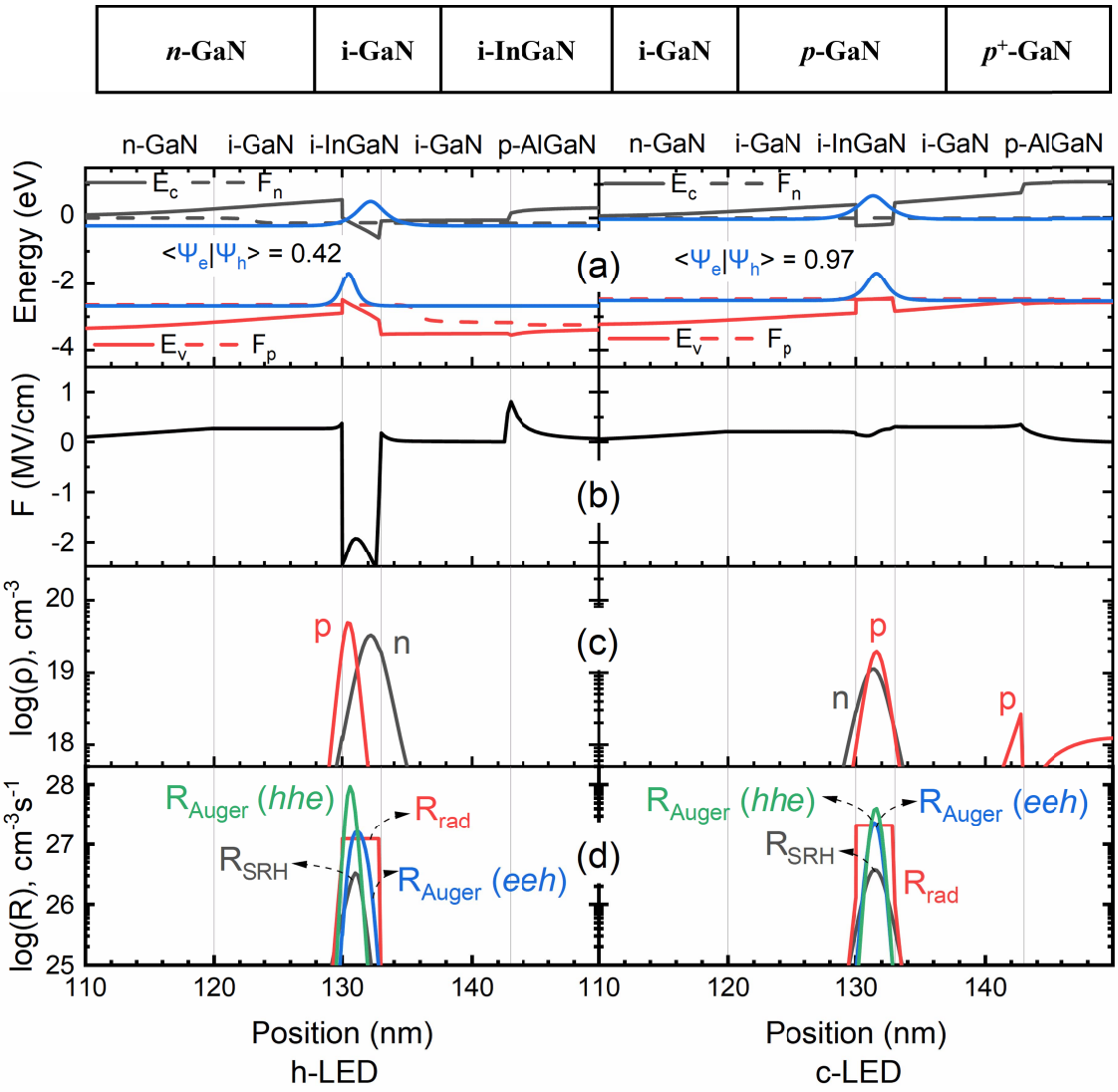

Fig. 1. Top schematic shows the device structure of the InGaAlN LEDs. (a) Band diagrams, (b) electric fields (F), (c) carrier concentrations (ρ), and (d) recombination rates (R) as a function of the position under the current density of 200 A/cm^2 for the h-LED and the c-LED are shown. The individual contributions of the recombination rates resulting from SRH (R_{SRH}), radiative (R_{rad}), eeh [R_{Auger}(eeh)], and hhe [R_{Auger}(hhe)] Auger recombination are also represented. The electron–hole wave function overlaps ($\langle\psi_e|\psi_h\rangle$) of h- and c-LEDs are 0.42 and 0.97, respectively. E_c, E_v, F_n, F_p, n, and p are conduction and valence band edges, quasi-Fermi levels for electron and hole, and electron and hole densities, respectively.

barrier/15-nm p-$Al_{0.2}Ga_{0.8}N$:Mg [Mg concentration of 5×10^{19} cm^{-3}]/100-nm-thick p-GaN:Mg [Mg concentration of 10^{19} cm^{-3}]/15-nm-thick p^+-GaN:Mg [Mg concentration of 10^{20} cm^{-3}]. A schematic of both LED structures is shown on top of Fig. 1. Simulations are carried out by the recently developed open-boundary quantum LED simulator (OBQ-LEDsim) [9], for which a trial wave function is introduced to describe the ground state of finite barrier QWs in the LED active layers in the presence of electric fields

$$\psi(x) = \sqrt{\frac{\beta^2}{2\pi\alpha}\sin\left(\frac{\alpha\pi}{\beta}\right)}\frac{e^{\alpha(x+\gamma)}}{\cosh[\beta(x+\gamma)]} \tag{1}$$

where α, β, and γ are variational parameters associated with the wave function symmetry, width, and position, respectively. The condition $\alpha < \beta$ ensures the trial wave function vanishes at infinity, without the need for artificial boundaries. This variational approach is integrated with the classical drift-diffusion model within the OBQ-LEDsim by solving the Schrödinger–Poisson equations self-consistently and updating the overall electric potentials with the quantum potentials through the Bohm potential technique [10]. Our approach merges nicely quantum and continuum physical quantities without enforcing artificial boundaries between the QW and classical continuum, thereby enabling quantum carrier densities to be explicitly defined at arbitrary positions in LEDs [11]. The software details have been reported in our earlier work [9], [11]. Carrier degeneracy and phase-space filling effects over the whole LED structures are considered by describing carrier densities using Fermi–Dirac statistics and by computing the spontaneous emission rates in the QW and the classical continuum with Fermi's golden rule, where the band-to-band optical transition matrix elements are derived from generalizing Kane's model [12], [13]. The calculated radiative

coefficients resulting from band-to-band recombination in h- and c-$In_{0.3}Ga_{0.7}N$ under nondegenerate conditions are 1.73×10^{-11} and 3.14×10^{-11} $cm^3 \cdot s^{-1}$, respectively. The former value agrees with the measured values ranging from 1.4×10^{-11} to 2×10^{-11} $cm^3 \cdot s^{-1}$, which validates the accuracy of the model [14]. The latter value is twice larger than the former value, implying that the radiative efficiency in c-InGaN is higher than in h-InGaN, which was confirmed by prior measurements [15]. We attribute the superior radiative efficiency of c-InGaN to the reduced electron and hole effective masses compared to those in h-InGaN counterparts [16]. For nonradiative recombination, we assume a Shockley–Read–Hall (SRH) nonradiative lifetime (τ) of 18.5 ns, eeh (C_n), and hhe (C_p) Auger coefficients of 10^{-30} $cm^6 \cdot s^{-1}$, while ohmic contacts are assumed for both LEDs [14], [17]–[19]. It should be pointed out that C_n and C_p in c-LEDs have not yet been reported in the literature. However, by comparing the electronic structure of c-GaN with that of h-GaN [17], [21], one can see that c-GaN has significantly fewer energy states close to the conduction band minimum and the valence band maximum. In particular, the energy difference between the first and second conduction bands at the Γ point is >8 eV [17], [20]. These effects combined are expected to impede both direct and indirect Auger transitions, leading to lower C_n and C_p with respect to h-GaN. In our analysis of the individual contributions of internal polarization and carrier effective mass to the efficiency droop, we use the same C_n and C_p in both LEDs, thereby underestimating the c-LED performances.

III. Results and Discussion

In Fig. 1(a)–(d), we show spatially resolved band diagrams, electric fields (F), carrier densities (ρ), and recombination rates (R) of the h- and c-LEDs operated under the same current density of 200 A/cm^2, respectively. As shown in Fig. 1(a) (left), the h-LED band edges tilt in the QW even with a high bias of 3.27 V. Polarization-induced electric fields are the major reason that prevents the h-LED from achieving flat-band conditions. The electrons and holes in the h-LED are strongly localized within their respective QW, resulting in a small electron–hole wave function overlap of 0.42, which is half of its value in the c-LED (right). As seen in Fig. 1(b) (left), the spatially separated QW electrons and holes screen the polarization-induced electric fields, yielding a 1.93-MV/cm electric field in the QW center, whereas the extension of the overall electric field toward the QW edges reaches a maximum value of 2.43 MV/cm. The c-LED exhibits a different effect, where the electric field achieves its minimum value of 0.13 MV/cm on the left QW edge and gradually increases to its maximum value of 0.31 MV/cm on the right QW edge. This severe field dissimilarity between the h- and c-phases is due to poor electron–hole wave function overlap caused by the presence of polarization field in the h-LED. Fig. 1(c) (left) shows the h-LED electrons and holes pile up in the QW, rising to peak densities of 3.30×10^{19} and 4.93×10^{19} cm^{-3}, respectively. These values are more than twice those in the c-LED (right). In the h-LED QW, the hole distribution is more localized than the electron distribution because the heavy hole mass (m_h^*) of 1.78 m_0 is ten times heavier than the electron effective mass (m_e^*) of 0.16 m_0 exhibiting a higher hole density peak than the electron density peak. It follows that the electron–hole wave function overlap in the QWs is influenced by the large m_h^*. Fig. 1(d) displays the effects of the poor electron–hole wave function overlap on SRH, radiative, eeh, and hhe Auger recombination. It is seen that the strong hole localization caused by the coexistence of strong internal polarization and large hole effective mass in the h-LED (left) boosts the peak hole density and enhances the hhe Auger recombination. Interestingly, the hhe Auger recombination rates overcome the SRH, radiative, and eeh Auger recombination rates, making it the dominant recombination channel because the hole distribution is more localized in the QW than the electron distribution. On the opposite, the electron–hole wave function overlap is enhanced in the c-LED (right) because of its polarization-free nature and its smaller hole effective mass, i.e., $m_h^* = 0.84\ m_0$. In conclusion, increasing the electron–hole wave function overlap lowers peak carrier densities, weakens Auger recombination asymmetry, and enhances the radiative recombination rate.

Fig. 2(a) shows the squared electron–hole wave function overlap ($|\langle\psi_e|\psi_h\rangle|^2$) and the peak emission wavelength as a function of current density for both the h- and c-LEDs. Under a typical operational current density of 35 A/cm^2, the squared electron–hole wave function overlap in the h-LED is 17% of that in the c-LED. As the current density increases to 200 A/cm^2, the h-LED value increases to 19% of that in the c-LED. As mentioned above, the squared electron–hole wave function overlap is significantly lower in the h-LED than in the c-LED regardless of current densities because of the strong polarization-induced electric fields. The peak emission wavelength of h-LED blueshifts from 518 to 509 nm as the current density increases from 1 to 200 A/cm^2. In contrast, c-LED emits at $\sim$502 nm with only a 0.2-nm blueshift for the same current density range. Fig. 2(b) shows electron and hole sheet charge densities (σ) in the QW as a function of current density for the h- and c-LEDs. The electron and hole sheet charge densities of h-GaN are more than two times larger than those in the c-LED. This is again attributed to the large internal polarization of the h-LED. As described earlier, large internal polarization causes poor electron–hole wave function overlap, which requires higher QW carrier densities to achieve the same total recombination rate as in the absence of internal polarization.

In order to identify the individual contributions of internal polarization and carrier effective mass to the efficiency droop, we simulated one additional structure, i.e., a nonpolar h-LED. The nonpolar h-LED has the same h-LED device structure, as described in Fig. 1 (left), but is grown on m-plane GaN substrates. Fig. 3 displays the normalized IQE and efficiency droop of the three LEDs as a function of current density. The h-LED suffers from the poorest electron–hole wave function overlap, resulting in the highest efficiency droop of 45% under 200 A/cm^2. The efficiency droop is reduced to 29% (i.e., a 35% reduction) for the nonpolar h-LED due to internal polarization elimination. It should be emphasized that

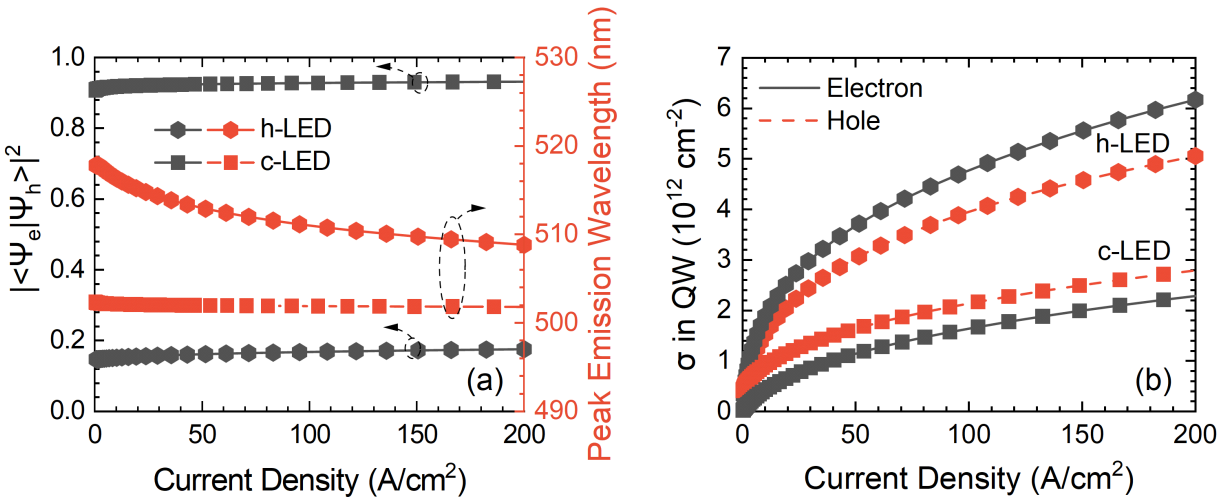

Fig. 2. (a) Squared electron–hole wave function overlap ($|\langle\psi_e|\psi_h\rangle|^2$) (left *y*-axis) and peak emission wavelength (right *y*-axis). (b) Electron and hole sheet charge densities (σ) in the QW as a function of current density for the h- and c-LEDs are shown.

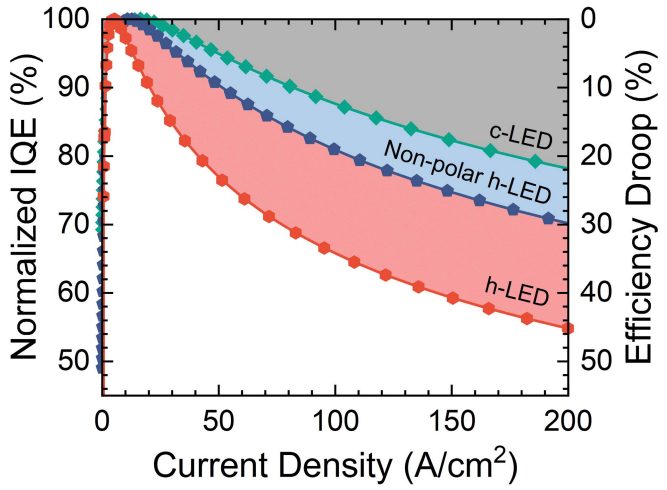

Fig. 3. Normalized IQE (left *y*-axis) and efficiency droop (right *y*-axis) as a function of current density are plotted. Red hexagons and green rhombuses refer to the h- and c-LEDs, whereas blue pentagons refer to the nonpolar h-LED grown on *m*-plane GaN substrates.

the efficiency droop reduction in nonpolar h-LEDs that was previously attributed to the decrease in the carrier leakage from active region overlooks the interplay between internal polarization and Auger recombination [22], [23]. Indeed, recent experiments suggest that the efficiency droop reduction in nonpolar h-LEDs is, in fact, due to carrier delocalization (a situation different than in polar h-LEDs) that results in stronger electron–hole wave function overlap, lower QW carrier densities, and lower Auger recombination rates [24]. Switching from nonpolar h-LEDs to c-LEDs further quenches the efficiency droop from 29% to 22% (i.e., a 24% reduction). This reduction is primarily due to the increased band-to-band optical transition matrix element and electron–hole wave function overlap. We attributed the increase in the band-to-band optical transition matrix element (electron–hole wave function overlap) to the decrease in m_e^* (m_h^*) from 0.16 (1.78) m_0 in the h-LED to 0.13 (0.84) m_0 in the c-LED. Overall, the efficiency droop in c-LEDs has been substantially reduced by ~51% with respect to the traditional h-LEDs by means of internal polarization elimination and carrier effective mass reduction. Such significant improvement indicates that the coexistence of strong internal polarization and large carrier effective mass is the major cause of the efficiency droop that cannot be solely explained by the large Auger coefficient.

One cannot emphasize more the role of internal polarization on the wave function overlap on the onset of Auger recombination and its effect on the IQE, which is missing in the well-known ABC model [25], for which $n = p$ is a common approximation without consideration for the electron–hole wave function overlap. Despite the fact that the effective ambipolar Auger coefficient (C_a) in QWs is calculated by multiplying the bulk C_a value by the squared electron–hole wave function overlap [26], prior studies have shown that disregarding this electron–hole wave function overlap would result in an overestimation of the C_a value [27]. This overestimation is observed in this study, where we consider the influence of the Auger electron–hole asymmetry ($C_n/C_p \neq 1$) on the efficiency droop. In a previous work, we reported that the efficiency droop significantly depends on the Auger electron–hole asymmetry [11]. Because the individual (C_n, C_p) coefficients are actually undetermined, we show in Fig. 4(a) and (b) the color plots of the efficiency droop as a function of C_n and C_p, separately, and expressed in units of 2×10^{-30} cm$^6 \cdot$s^{-1}, under the current density of 200 A/cm^2 for the h- and c-LEDs, respectively. C_a expressed in units of 2×10^{-30} cm$^6 \cdot$s^{-1} is shown as the dotted lines on these color plots. The efficiency droops of 45% and 22% for the h- and c-LEDs indicated by the dashed lines are chosen as references. They are calculated assuming the Auger electron–hole symmetry ($C_n/C_p = 1$) and $C_a = 2 \times 10^{-30}$ cm$^6 \cdot$s^{-1}. It is seen that multiple combinations of (C_n, C_p) result in the same efficiency droop. Hence, in the h-LED, this can be obtained by either decreasing or increasing C_n/C_p and C_a simultaneously. In the c-LED, it is seen that this behavior is not observed as the efficiency droop depends solely on C_a regardless of the C_n/C_p ratio.

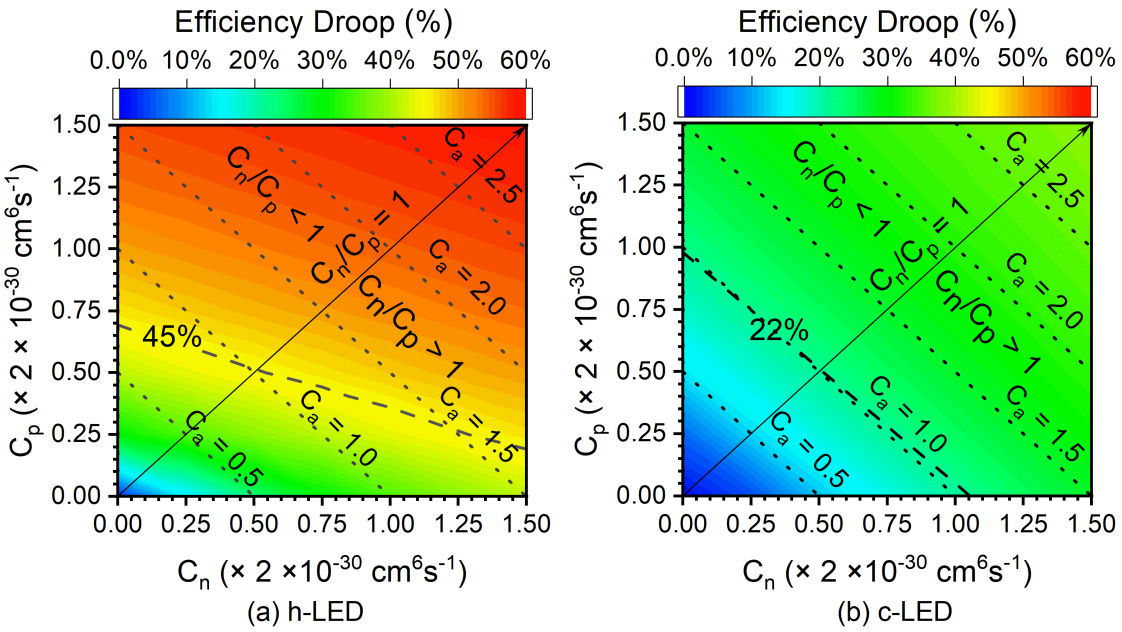

Fig. 4. Contour plots of the efficiency droop as a function of eeh (C_n) and hhe (C_p) Auger coefficients under the current density of 200 A/cm^2 for (a) h-LED and (b) c-LEDs are shown. The ambipolar Auger coefficient (C_a) expressed in units of 2×10^{-30} cm$^6 \cdot$s^{-1} is shown as the dotted lines. The efficiency droops of 45% and 22% for the h- and c-LEDs are indicated by the dashed lines, respectively. They are calculated assuming Auger electron–hole symmetry ($C_n/C_p = 1$) and $C_a = 2 \times 10^{-30}$ cm$^6 \cdot$s^{-1} and highlighted as references.

This behavior difference between the h-LED and the c-LED is credited to strong Auger recombination asymmetry in h-LEDs, as explained in Fig. 1. As a result, an optimum C_n/C_p ratio in the h-LED could reduce the efficiency droop from 51% to 35% if $C_a = 2 \times 10^{-30}$ cm$^6 \cdot$s^{-1}. It is also pointed out that the impact of C_n/C_p uncertainty on the efficiency droop increases with increased C_a. Therefore, it appears highly improbable that, in h-LEDs, the efficiency droop is attributed to a single C_a value, without considering the impact of the electron–hole wave function overlap on the recombination mechanism. Asides from this later point, one can then conclude that the h-LEDs tend to exhibit stronger efficiency droop than c-LEDs with C_a increase. For instance, the h- and c-LEDs have both vanishing efficiency droop for $C_n = C_p = 0$ cm$^6 \cdot$s^{-1}. Yet, for $C_n = C_p = 3 \times 10^{-30}$ cm$^6 \cdot$s^{-1}, the efficiency droop in h-LED can reach up to 59%, which is nearly twice the 38% observed in the c-LED. In addition, the fact that usual IQE degradations associated with defects, phonons, alloy disorders, and interface roughness [4] are commonly linked to the increase in C_a implies that the efficiency droop in h-LED is more sensitive to these degradation mechanisms than the c-LED. For these reasons, c-LEDs offer an appropriate solution to reduce the impact of these degradation effects on the efficiency droop, resulting in more efficient green LEDs than h-LEDs. Moreover, in h-LEDs, wavelengths longer than blue (i.e., >450 nm) are achieved by increasing the indium composition in the QW. This process, unfortunately, further enhances internal polarization, increases hole effective mass, and deteriorates electron–hole wave function overlap, which explains why green LEDs have stronger efficiency droop than blue ones.

IV. Conclusion

In conclusion, the OBQ-LEDsim-based analysis confirms that a large electron–hole wave function overlap is critical for achieving optimal IQE in green LEDs. It is shown that, in c-LEDs, the absence of internal polarization combined with the existence of small carrier effective mass contributes to enhancing electron–hole wave function overlap and lowering carrier densities, thereby quenching the efficiency droop. These results indicate that the major cause of the efficiency degradation in green h-LEDs is the poor electron–hole wave function overlap and cannot be explained by the sole Auger coefficient value. In this context, the well-known ABC model may inadvertently overestimate the Auger coefficient by overlooking the electron–hole wave function overlap, which leads to incorrect conclusions on the efficiency droop. In contrast, the c-LED efficiency droop is much immune to the indetermination of the Auger electron–hole asymmetry and the increase in the ambipolar Auger coefficient value and is also more robust to the adverse effects of efficiency degradation mechanisms. Based on these considerations, one may surmise that the absence of internal polarization and small carrier effective mass found in c-LEDs would result in increased current density at the onset of the efficiency droop and reduce the efficiency droop by ~51% (w.r.t. h-LEDs) under high current densities. Introducing more QWs in c-LEDs could further reduce QW carrier densities and quench the efficiency droop since carrier delocalization and homogeneous injection are enabled in multiple QWs by the lack of internal polarization and carrier effective mass reduction.

REFERENCES

[1] M. Pattison *et al.*, "2019 lighting R&D opportunities," Solid State Lighting Solutions (SSLS) Inc. Santa Barbara, CA, USA, Tech. Rep. DOE/EE-2008, Jan. 2020, doi: 10.2172/1618035.

[2] A. L. Hicks, T. L. Theis, and M. L. Zellner, "Emergent effects of residential lighting choices: Prospects for energy savings," *J. Ind. Ecol.*, vol. 19, no. 2, pp. 285–295, Apr. 2015, doi: 10.1111/JIEC.12281.

[3] J. Iveland, L. Martinelli, J. Peretti, J. S. Speck, and C. Weisbuch, "Direct measurement of Auger electrons emitted from a semiconductor light-emitting diode under electrical injection: Identification of the dominant mechanism for efficiency droop," *Phys. Rev. Lett.*, vol. 110, no. 17, Apr. 2013, Art. no. 177406, doi: 10.1103/PhysRevLett.110.177406.

[4] E. Kioupakis, D. Steiauf, P. Rinke, K. T. Delaney, and C. G. Van de Walle, "First-principles calculations of indirect Auger recombination in nitride semiconductors," *Phys. Rev. B, Condens. Matter*, vol. 92, no. 3, Jul. 2015, Art. no. 035207, doi: 10.1103/PhysRevB.92.035207.

[5] C.-K. Tan, W. Sun, J. J. Wierer, and N. Tansu, "Effect of interface roughness on Auger recombination in semiconductor quantum wells," *AIP Adv.*, vol. 7, no. 3, Mar. 2017, Art. no. 035212, doi: 10.1063/1.4978777.

[6] J. Cho, E. F. Schubert, and J. K. Kim, "Efficiency droop in light-emitting diodes: Challenges and countermeasures," *Laser Photon. Rev.*, vol. 7, no. 3, pp. 408–421, May 2013, doi: 10.1002/lpor.201200025.

[7] R. Windisch *et al.*, "40% efficient thin-film surface-textured light-emitting diodes by optimization of natural lithography," *IEEE Trans. Electron Devices*, vol. 47, no. 7, pp. 1492–1498, Jul. 2000, doi: 10.1109/16.848298.

[8] J. Wang, P. von Allmen, J.-P. Leburton, and K. J. Linden, "Auger recombination in long-wavelength strained-layer quantum-well structures," *IEEE J. Quantum Electron.*, vol. 31, no. 5, pp. 864–875, May 1995, doi: 10.1109/3.375931.

[9] Y.-C. Tsai, C. Bayram, and J.-P. Leburton. (2021). *An Open Boundary Quantum LED Simulator (OBQ-LEDsim)*. [Online]. Available: http://obqledsim.ece.illinois.edu/

[10] C. de Falco, E. Gatti, A. L. Lacaita, and R. Sacco, "Quantum-corrected drift-diffusion models for transport in semiconductor devices," *J. Comput. Phys.*, vol. 204, no. 2, pp. 533–561, Apr. 2005, doi: 10.1016/j.jcp.2004.10.029.

[11] Y.-C. Tsai, C. Bayram, and J.-P. Leburton, "Effect of Auger electron–hole asymmetry on the efficiency droop in InGaN quantum well light-emitting diodes," *IEEE J. Quantum Electron.*, vol. 58, no. 1, pp. 1–9, Feb. 2022, doi: 10.1109/JQE.2021.3137822.

[12] S. L. Chuang, "Optical gain of strained wurtzite GaN quantum-well lasers," *IEEE J. Quantum Electron.*, vol. 32, no. 10, pp. 1791–1800, Oct. 1996, doi: 10.1109/3.538786.

[13] S. L. Chuang, *Physics of Photonic Devices*, 2nd ed. Hoboken, NJ, USA: Wiley, 2009.

[14] Y. C. Shen, G. O. Mueller, S. Watanabe, N. F. Gardner, A. Munkholm, and M. R. Krames, "Auger recombination in InGaN measured by photoluminescence," *Appl. Phys. Lett.*, vol. 91, no. 14, Oct. 2007, Art. no. 141101, doi: 10.1063/1.2785135.

[15] R. Liu, R. Schaller, C. Q. Chen, and C. Bayram, "High internal quantum efficiency ultraviolet emission from phase-transition cubic GaN integrated on nanopatterned Si(100)," *ACS Photon.*, vol. 5, no. 3, pp. 955–963, Mar. 2018, doi: 10.1021/acsphotonics.7b01231.

[16] T. Trupke and M. A. Green, "Temperature dependence of the radiative recombination coefficient of intrinsic crystalline silicon," *J. Appl. Phys.*, vol. 94, no. 8, pp. 4930–4937, Oct. 2003, doi: 10.1063/1.1610231.

[17] Y.-C. Tsai and C. Bayram, "Structural and electronic properties of hexagonal and cubic phase AlGaInN alloys investigated using first principles calculations," *Sci. Rep.*, vol. 9, no. 1, p. 6583, Dec. 2019, doi: 10.1038/s41598-019-43113-w.

[18] Y.-C. Tsai and C. Bayram, "Band alignments of ternary Wurtzite and zincblende III-nitrides investigated by hybrid density functional theory," *ACS Omega*, vol. 5, no. 8, pp. 3917–3923, Mar. 2020, doi: 10.1021/acsomega.9b03353.

[19] Y.-C. Tsai and C. Bayram, "Mitigate self-compensation with high crystal symmetry: A first-principles study of formation and activation of impurities in GaN," *Comput. Mater. Sci.*, vol. 190, Apr. 2021, Art. no. 110283, doi: 10.1016/j.commatsci.2021.110283.

[20] K. T. Delaney, P. Rinke, and C. G. Van de Walle, "Auger recombination rates in nitrides from first principles," *Appl. Phys. Lett.*, vol. 94, no. 19, May 2009, Art. no. 191109, doi: 10.1063/1.3133359.

[21] R. B. Araujo, J. S. de Almeida, and A. F. da Silva, "Electronic properties of III-nitride semiconductors: A first-principles investigation using the Tran–Blaha modified Becke–Johnson potential," *J. Appl. Phys.*, vol. 114, no. 18, Nov. 2013, Art. no. 183702, doi: 10.1063/1.4829674.

[22] J. Piprek and S. Li, "Electron leakage effects on GaN-based light-emitting diodes," *Opt. Quantum Electron.*, vol. 42, no. 2, pp. 89–95, Jan. 2010, doi: 10.1007/s11082-011-9437-z.

[23] D. Saguatti *et al.*, "Investigation of efficiency-droop mechanisms in multi-quantum-well InGaN/GaN blue light-emitting diodes," *IEEE Trans. Electron Devices*, vol. 59, no. 5, pp. 1402–1409, May 2012, doi: 10.1109/TED.2012.2186579.

[24] M. Shahmohammadi *et al.*, "Enhancement of Auger recombination induced by carrier localization in InGaN/GaN quantum wells," *Phys. Rev. B, Condens. Matter*, vol. 95, no. 12, pp. 1–10, Mar. 2017, doi: 10.1103/PhysRevB.95.125314.

[25] H. Y. Ryu, H. S. Kim, and J. I. Shim, "Rate equation analysis of efficiency droop in InGaN light-emitting diodes," *Appl. Phys. Lett.*, vol. 95, no. 8, pp. 8–11, 2009, doi: 10.1063/1.3216578.

[26] E. Kioupakis, Q. Yan, D. Steiauf, and C. G. Van de Walle, "Temperature and carrier-density dependence of Auger and radiative recombination in nitride optoelectronic devices," *New J. Phys.*, vol. 15, Dec. 2013, Art. no. 125006, doi: 10.1088/1367-2630/15/12/125006.

[27] J. Piprek, F. Römer, and B. Witzigmann, "On the uncertainty of the Auger recombination coefficient extracted from InGaN/GaN light-emitting diode efficiency droop measurements," *Appl. Phys. Lett.*, vol. 106, no. 10, Mar. 2015, Art. no. 101101, doi: 10.1063/1.4914833.